EPJ AP

Applied Physics

EPJ.org

your physics journal

Eur. Phys. J. Appl. Phys. **81**, 11101 (2018) **DOI:** 10.1051/epjap/2017170332

# Experimental study of light emitted by spark-generated bubbles in water

Karel Vokurka and Silvano Buogo

edp sciences

The title “The European Physical Journal” is a joint property of EDP Sciences, Società Italiana di Fisica (SIF) and Springer

Eur. Phys. J. Appl. Phys. **81**, 11101 (2018)

https://doi.org/10.1051/epjap/2017170332

THE EUROPEAN PHYSICAL JOURNAL APPLIED PHYSICS

Regular Article

# Experimental study of light emitted by spark-generated bubbles in water

Karel Vokurka[1,*] and Silvano Buogo[2]

[1] Physics Department, Technical University of Liberec, Studentská 2, 46117 Liberec, Czech Republic
[2] CNR-INSEAN, Marine Technology Research Institute, Via di Vallerano 139, 00128 Roma, Italy

Received: 25 September 2017 / Accepted: 24 November 2017

**Abstract.** The emission of light from spark-generated bubbles freely oscillating in water far from boundaries is studied experimentally. The observations concentrate on light flashes radiated at final stages of the first bubble contraction and early stages of the following bubble expansion. It is shown that the shape of the emitted light pulses is not "Gaussian", but asymmetric with a leading edge moderately growing and a trailing edge steeply decreasing. The maximum values and widths of these optical pulses are determined for bubbles having different sizes and oscillating with different intensities. The variation of the maximum values and pulse widths with bubble size and intensity of oscillation is discussed, as well as the observed weak correlation between these two quantities.

## 1 Introduction

Bubble oscillations have long been an important topic in fluid dynamics. While they have been traditionally associated with erosion damage [1,2], recent efforts have been aimed at medical applications, such as contrast-enhancing in ultrasonic imaging [3–6], ultrasound therapy monitoring [7], and shock wave lithotripsy [8]. In experimental studies of free bubble oscillations both spark-generated bubbles [9–11] and laser-generated bubbles [12] represent very useful tools.

Light emission from bubbles oscillating in liquids has been studied extensively in experiments where bubbles are generated using a wide variety of techniques. These techniques include single bubbles oscillating in acoustic resonators [13–15], multiple bubbles oscillating in variable pressure fields [16–19], laser-generated bubbles [20–24], spark-generated bubbles [25–29], steam bubbles [30], and shock induced collapse [31]. For a review of literature on light emission from bubbles see also Yasui et al. [32]. Despite these efforts, however, the mechanism of light emission is not well understood yet. The reason for this still limited understanding can be seen in complex physical processes running very fast in the bubble interior for a short time interval and hence in difficulties associated with studying these processes experimentally.

At present there are two predominant methods used to study emission of light from bubbles. In works [21,23,25] optical spectra of light flashes have been determined. It has been found out that in the case of spark and laser-generated bubbles the spectra are continuous and the corresponding temperatures of the plasma core estimated using the Wien and Plank law range from 5800 K to 8150 K [21,23,25]. In other works [13–18,21–23] shapes of the light flashes have been studied. It has been found out that the waveform of light pulses is "Gaussian" and the widths of the pulses range from 150 ps to 9 ns [13–15,21–23]. However, in works [13–15] the widths of light pulses have been reported without giving the size and intensity of oscillation of the bubbles. And in works [21–23] only the variation of the pulse widths with bubble size is given, but no variation of the pulse widths with bubble oscillation intensity is presented. The dependency of the maximum values of the light pulses with bubble size and bubble oscillation intensity has not been reported in the literature yet.

In this work results obtained in experiments with large spark-generated bubbles freely oscillating in water far from boundaries are given. An obvious advantage of large bubbles is that optical and acoustic radiation from them can be recorded more easily than in the case of smaller bubbles. This is because in large oscillating bubbles physical processes are taking place more slowly. Light emitted by large bubbles is also sufficiently intensive so that averaging on light pulses from different experiments, which is always accompanied by a loss of natural variety (e.g., in pulse shape), is not necessary. Photographs of large bubbles also reveal details not easily seen in the case of small bubbles. The technique of low voltage spark discharges makes it also possible to generate bubbles of different sizes and oscillating with different intensities [33], which further enhance the data analysis. The most important findings presented in this work can be summarized as follows. First, we attempt to show that the light is emitted from a glowing plasma core in the bubble interior during the whole first bubble oscillation and not only at the final stages of the bubble contraction and at early stages of the following bubble expansion. We also show that in the

* e-mail: karel.vokurka@tul.cz

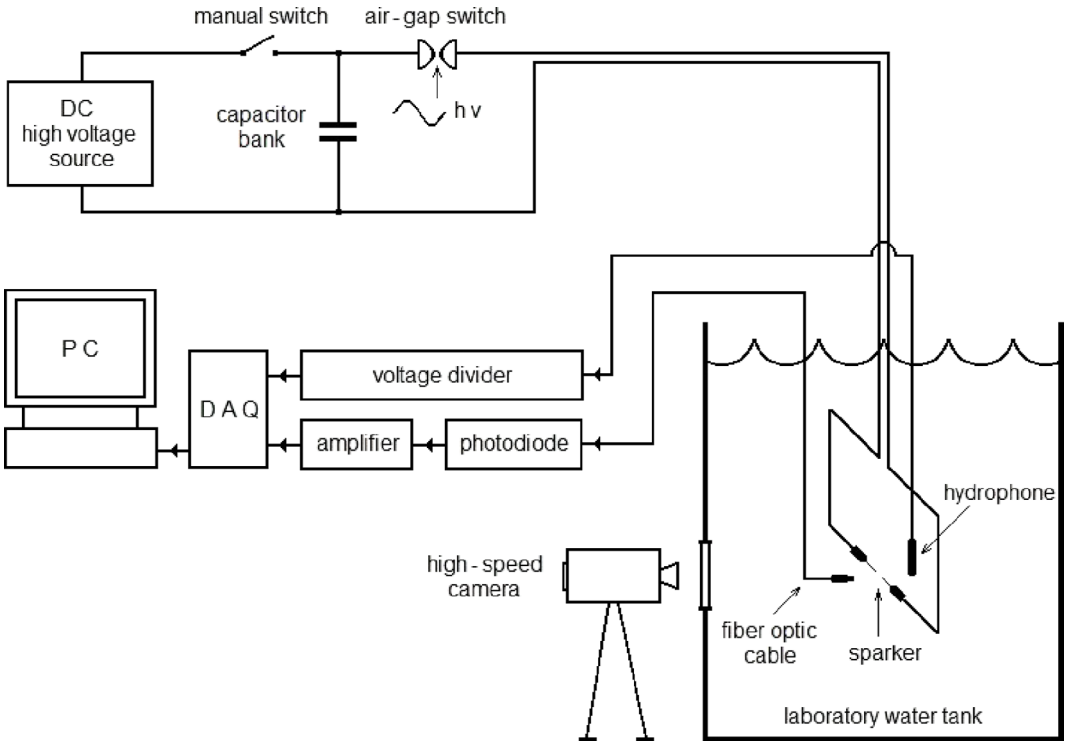


**Fig. 1.** Experimental setup used to generate oscillating bubbles and record optical and acoustic radiation from them (abbreviations in the figure: DAQ − data acquisition board, hv − additional high voltage used to trigger the air gap).

case of spark-generated bubbles the shape of the optical pulse is not "Gaussian", as reported in works [13–18,21–23], but rather is asymmetric with a leading edge growing relatively slowly and a trailing edge decreasing abruptly. Finally, we present the variation of the maximum values and widths of optical pulses with both the bubble size and bubble oscillation intensity. After analysing data obtained on a large set of spark-generated bubbles, it is concluded that the scaling law cannot be applied to the maximum surface temperatures of the plasma core and that the plasma core inside the bubbles behaves rather autonomously with respect to the pressure at the bubble wall. This second conclusion is possible because not only the bubble size, but also the bubble oscillation intensity is determined in each experiment. Results discussed here are an extension of earlier works presented at conferences [34,35].

## 2 Experimental setup

The experimental setup used in this work is schematically shown in Figure 1. Freely oscillating bubbles were generated by discharging a capacitor bank via a sparker submerged in a laboratory water tank having dimensions of 6 m (length) $\times$ 4 m (width) $\times$ 5.5 m (depth). The experiments were performed in tap water at a constant hydrostatic pressure $p_\infty = 125$ kPa, at a room temperature $\Theta_\infty = 292$ K, and far from any boundaries. The capacitance of the capacitor bank could be varied in steps by connecting 1–10 capacitors in parallel. Each of these capacitors had a capacitance of 16 $\mu$F. The capacitors were charged from a high voltage source of 4 kV. An air-gap switch was used to trigger the discharge through the sparker. Earlier measurements [36] have shown that the current flowing through the discharge circuit has the form of a highly damped sinusoid and depending on the total bank capacity it drops to zero in 0.3–0.7 ms after the liquid breakdown. A more detailed description of the experimental setup is given in an earlier work [36].

Both the spark discharge and subsequent bubble oscillations were accompanied by intensive optical and acoustic radiations. The optical radiation was monitored by a detector, which consisted of a fibre optic cable, photodiode, amplifier, and A/D converter. The input surface of the fibre optic cable was positioned in water at the same level as the sparker at a distance $r = 0.2$ m aside, pointing perpendicularly to the sparker gap and the electrodes. At the output surface of the fibre optic cable a Hammamatsu photodiode type S2386-18L was positioned. The usable spectral range of the photodiode is 320–1100 nm. The analysis of the optical spectra given in literature has shown that the maximum temperatures in spark and laser-generated bubbles range from 5800 K to 8150 K [21,23,25]. Then by using the Wien and Planck law it can be verified that the spectral maxima of the optical radiation are within the photodiode bandpass and that the prevailing part of radiation is received by the detector. The load resistance of the photodiode was 75 $\Omega$, thus the rise time of the measured pulses is about 50 ns. A broadband amplifier (0–10 MHz) was connected to the photodiode output terminals. The output voltage from the amplifier was recorded using a data acquisition board (National instruments PCI 6115, 12 bit A/D converter) with a sampling frequency of 10 MHz. The presented optical data are referring to the photodiode output.

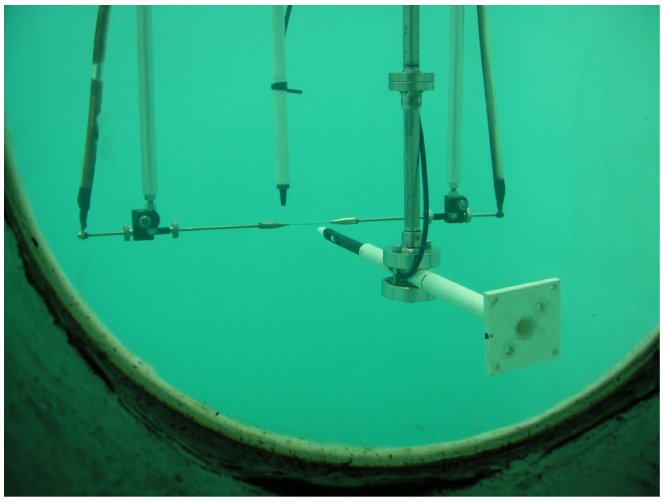

**Fig. 2.** A view through the observation window at the sparker, hydrophone and fibre optic cable submerged in water.

The acoustic radiation was monitored with a reson broadband hydrophone type TC 4034. The hydrophone was positioned with the sensitive element at the same depth as the sparker. The distance between the hydrophone acoustic centre and the sparker gap was $r_h = 0.2$ m. The output of the hydrophone was connected via a divider 10:1 to the second channel of the A/D converter. The configuration of the sparker, hydrophone and fibre optic cable terminal submerged in water can be seen in a photograph in Figure 2.

In the experiments a large number of almost spherical bubbles (bubbles are slightly elongated in a vertical direction [33]) freely oscillating in a large expanse of liquid were successively generated. The sizes of these bubbles, as described by the first maximum radius $R_{M1}$, ranged from 18.5 mm to 56.5 mm, and the bubble oscillation intensity, as described by the non-dimensional peak pressure [33]

$$p_{zp1} = \frac{p_{p1}}{p_\infty}\frac{r_h}{R_{M1}}, \qquad (1)$$

ranged from 24 to 153. Here $p_{p1}$ is the peak pressure in the acoustic pulse $p_1(t)$. The quantity $p_{zp1}$ can be best interpreted as the peak acoustic pressure in the pulse $p_1(t)$ measured at a distance $r_h = R_{M1}$ and divided by the hydrostatic pressure $p_\infty$. Both $R_{M1}$ and $p_{zp1}$ were determined in each experiment from the respective pressure record using an iterative procedure described in detail in [33]. This iterative procedure is an extension of the well-known Rayleigh's formula for the "collapse time" of a bubble having a size $R_{M1}$. The Rayleigh formula is commonly used in studies of spark and laser-generated bubbles (see, e.g. [21,23]). It has been verified experimentally many times that for bubbles oscillating sufficiently intensively it gives satisfactory results (see, e.g. Fig. 6 in [1]). However, for bubbles oscillating with lower intensity it gives less precise values. The iterative procedure is extending this approach to any oscillation intensity.Prior to the measurements reported here a limited number of high-speed camera records were taken with framing rates ranging from 2800 frames/s to 3000 frames/s. These records were used to check the shape of the generated bubbles and the photographs yielded also useful visual information on the bubble content. Examples of several frames from one film record corresponding to different times are given in Figure 3.

In Figure 3 the first frame was taken during the bubble growth phase and the second frame shows the bubble slightly after time $t_1$ when it attained the first maximum radius $R_{M1}$. The third to sixth frames correspond to the first contraction phase and the seventh and eighth frames correspond to the first expansion phase. The sixth frame was taken shortly before the bubble was contracted at the instant $t_{c1}$ to the first minimum radius $R_{m1}$, the seventh frame corresponds to an instant shortly after $t_{c1}$ and the eighth frame was taken shortly after time $t_2$ when the bubble attained its second maximum radius $R_{M2}$. The small bright objects floating in the vicinity of the bubble are plasma packets [37]. The glowing plasma core in the bubble interior can be seen in the frames taken during the growth and first contraction phases.

As can be seen in the photographs in Figure 3, a glowing plasma core is present in the bubble during the whole first oscillation and emits light. This fact has motivated us to monitor the light emission from the plasma core in a greater detail. The results thus obtained are given in Section 3.

## 3 Results

An example of optical record, represented by the voltage $u(t)$ at the output of the optical detector, is given in Figure 4. The optical record consists of the pulse $u_0(t)$ that is radiated during the electric discharge and the following explosive bubble growth, and of the pulse $u_1(t)$ that is radiated during the first bubble contraction and the following bubble expansion.

This work is devoted to studying the pulse $u_1(t)$ only, and therefore the pulse $u_0(t)$ is shown clipped in Figure 4. The maximum value of the pulse $u_1(t)$ has been denoted as $u_{M1}$ and the time of its occurrence as $t_{u1}$. An interesting fact which can be seen in Figure 4 is the occurrence of optical radiation from the bubble during the whole first oscillation, that is, at the interval lasting approximately $(0, t_{u1})$. As can be observed in the photographs given in Figure 3, the source of this persisting optical radiation is a glowing plasma core. It can also be seen in these photographs that the bubble interior is filled with two substances. The first one is a transparent matter, which is, most probably, hot water vapour. The second one is opaque plasma at the bubble centre. The presence of this hot plasma core during the whole first bubble oscillation, that is, even long after the electric discharge has terminated (in case of the experimental data shown in Figs. 3 and 4 the electric discharge lasted approximately only 500 μs) is an astonishing phenomenon observed already by Golubnichii et al. [27,28]. Golubnichii et al. [27,28] called this persisting plasma core "the long-living luminescence formations". Similar long lasting optical radiation has also been observed by Baghdassarian et al. (see Fig. 1 in [21]). Baghdassarian et al. [21] explain this radiation as the "luminescence from metastable atomic and molecular

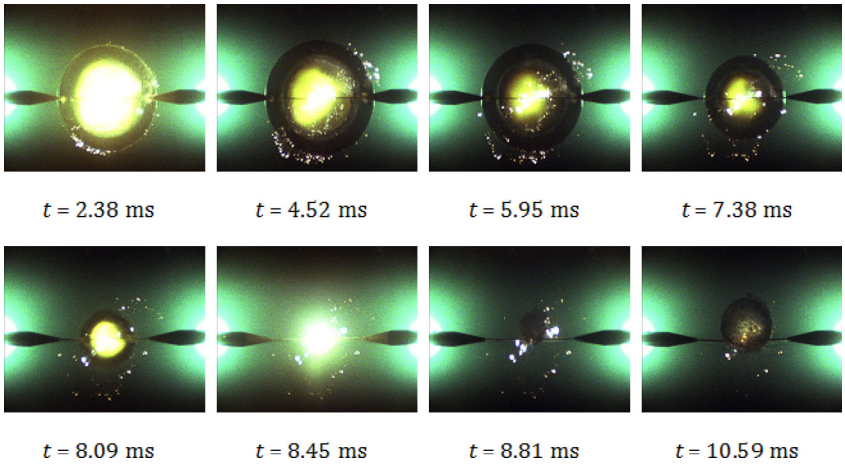


**Fig. 3.** Selected frames from a film record of a spark-generated bubble. The bubble has a size $R_{M1} = 51.5$ mm, and oscillates with an intensity $p_{zp1} = 70.3$. The times below each frame refer to the time origin which is set at the instant of the liquid breakdown. The light spots at the frame's sides are due to illuminating lamps.

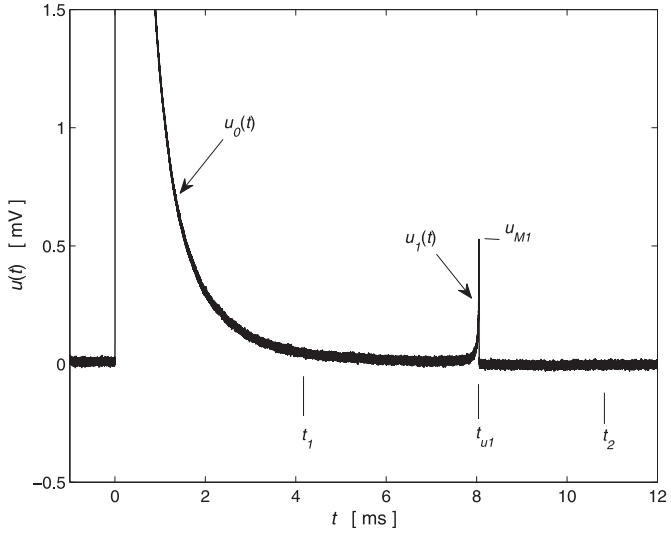


**Fig. 4.** Voltage $u(t)$ at the output of the optical detector. The spark-generated bubble has the size $R_{M1} = 49$ mm, and oscillates with the intensity $p_{zp1} = 142.1$. In this figure the time origin is set at the instant of the liquid breakdown and this instant coincides with the beginning of the rapid growth of pulse $u_0(t)$. The time when the bubble attains the first maximum radius $R_{M1}$ is denoted as $t_1$ and the time the bubble attains the second maximum radius $R_{M2}$ as $t_2$. The pulse $u_0(t)$ is defined to be within the interval (0, $t_1$), the pulse $u_1(t)$ within the interval ($t_1$, $t_2$).

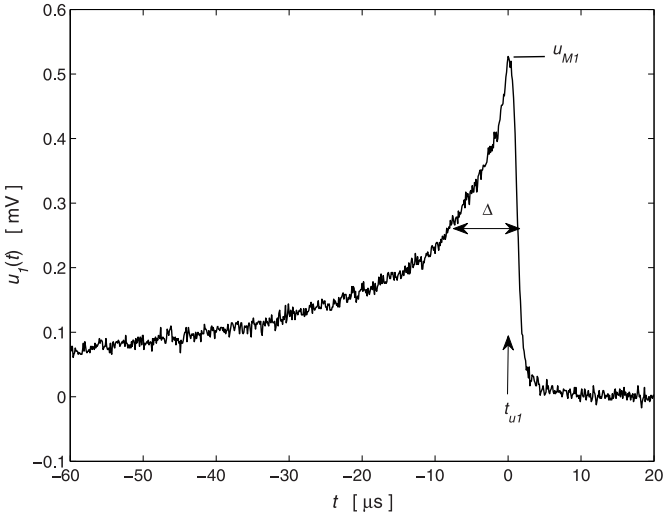


**Fig. 5.** A detailed view on the pulse $u_1(t)$ at the output of the optical detector. The spark-generated bubble has the size $R_{M1} = 49$ mm, and oscillates with the intensity $p_{zp1} = 142.1$. In this figure the time origin is set at the instant $t_{u1}$ and from the pulse $u_1(t)$ only a small portion near $t_{u1}$ is shown.

states injected into the water during or just after the plasma flash, which then recombine very slowly". However, it can be seen in Figure 3 that the light is emitted from the bubble interior and not from the surrounding water. A direct comparison of Figure 4 with Figure 1 in [21] can also be used as another proof that both in spark and laser-generated bubbles the glowing plasma core is present in their interior during the whole first bubble oscillation. And since there is no discharge current flowing through the laser-generated bubbles, then it follows that the persisting plasma core in spark-generated bubbles is not due to a persisting discharge current. However, as it will be shown later, a difference between the two kinds of bubbles exists, e.g. in the shape of the optical pulse, or in the variation of the optical pulse widths with the bubble size.

A detailed view on the pulse $u_1(t)$ is given in Figure 5. In Figure 5 only a small portion near $t_{u1}$ extracted from the whole pulse $u_1(t)$ is displayed and together with the maximum value $u_{M1}$ also the pulse full width $\Delta$ at one-half of the maximum value (i.e., at $u_{M1}/2$) is shown. As can also be seen in Figure 5, the intensity of optical radiation from the bubble increases relatively slowly to the maximum value $u_{M1}$ at $t_{u1}$ and then decreases to zero abruptly.

The energy spectral density level $L_{esd}$ of the pulse $u_1(t)$ is given in Figure 6. It can be seen from this spectrum that the rise time of the photodiode and the

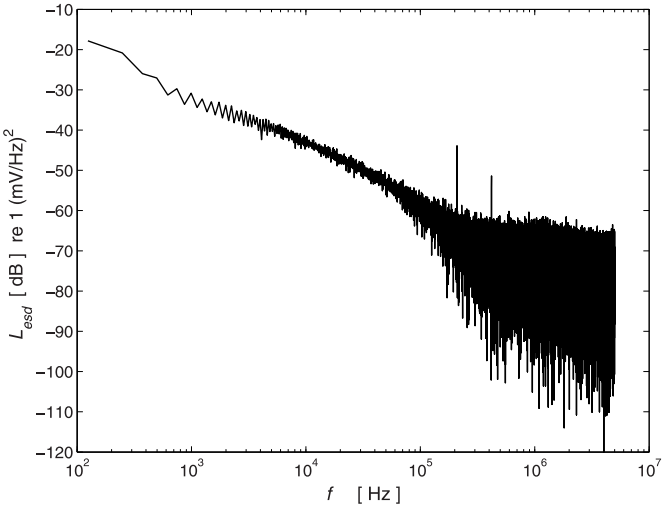


**Fig. 6.** The energy spectral density level $L_{esd}$ of the pulse $u_1(t)$. The spark-generated bubble had the size $R_{M1} = 49$ mm, and oscillated with the intensity $p_{zp1} = 142.1$. The energy spectral density, referred to 1 $(\mathrm{mV/Hz})^2$, has been computed for the pulse $u_1(t)$ in the time interval from $t_1$ to $t_2$.

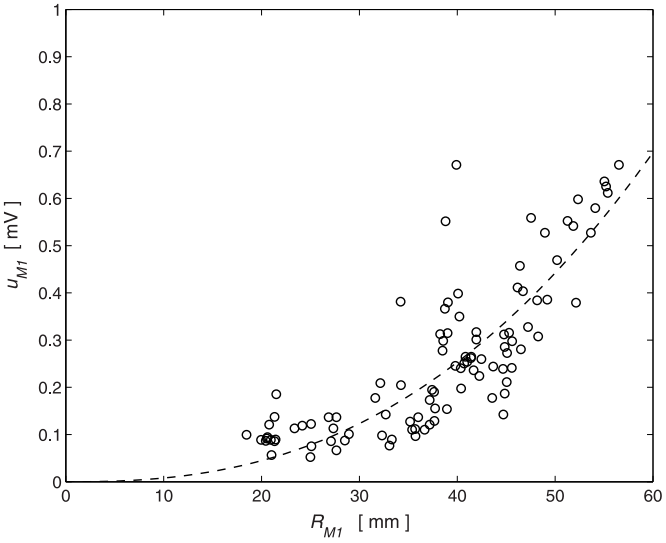


**Fig. 7.** The variation of the maximum voltage in the pulse, $u_{M1}$, with the bubble size, $R_{M1}$.

frequency and dynamic ranges of the optical detector were sufficient to record the pulse $u_1(t)$ in our experiments reliably.

The experiments were repeated many times and thus it was possible to record the pulses $u_0(t)$ and $u_1(t)$ for different bubble sizes, $R_{M1}$, and different intensities of oscillations, $p_{zp1}$. From the records of the pulses $u_0(t)$ and $u_1(t)$ a number of quantities can be determined. It has been shown earlier [37] that by analysing the energy partition in spark-generated bubbles, and the acoustic and optical radiations from these bubbles in particular, useful estimates of the plasma core surface temperatures $\Theta$ can be obtained. Using this method, the variation with the bubble size, $R_{M1}$, and oscillation intensity, $p_{zp1}$, of the plasma core surface temperature reached at the final stages of the bubble contraction, $\Theta_{M1}$, has been calculated, presented and discussed in reference [38]. In the present work, the form of the optical pulses $u_1(t)$ will be studied. From the many quantities describing the form of these pulses we want to concentrate on two of them. These are the maximum voltage in the pulse $u_{M1}$ and the pulse full width $\Delta$ at one-half of the maximum value. The analysis of several other interesting quantities will be presented elsewhere.

The variation of the maximum voltage in the pulse, $u_{M1}$, with the bubble size, $R_{M1}$, is shown in Figure 7. The nonlinear regression fit to this data is $<u_{M1}> = 2.5 \times 10^{-5}$ ${R_{M1}}^{2.5}$ [mV, mm].

The variation of the maximum voltage in the pulse, $u_{M1}$, with the bubble oscillation intensity, $p_{zp1}$, is shown in Figure 8. The nonlinear regression fit to this data is $<u_{M1}> = 3.5 \times 10^{-4}$ ${p_{zp1}}^{1.4}$ [mV, −].

The variation of the pulse width, $\Delta$, with the bubble size, $R_{M1}$, is shown in Figure 9. The nonlinear regression fit to this data is $<\Delta> = 1.1 \times 10^{-4}$ ${R_{M1}}^{3.3}$ [μs, mm].

The variation of the pulse width, $\Delta$, with the bubble oscillation intensity, $p_{zp1}$, is shown in Figure 10. The nonlinear regression fit to this data is $<\Delta> = 23.7$ ${p_{zp1}}^{0}$ [μs, −].

## 4 Discussion

In Section 3 it has been shown that the time dependence of the intensity of light emitted from a freely oscillating spark-generated bubble during its first contraction and its following expansion has a specific shape. In this work the intensity of light has been represented by voltage at the output from the photodiode and the form of the corresponding voltage pulse $u_1(t)$ has been displayed in Figure 4 and in detail in Figure 5. The shape of this pulse is relatively well reproducible in repeated experiments. However, if the maximum values $u_{M1}$ of the pulses $u_1(t)$, and their widths $\Delta$ are investigated on a larger set of data, it can be seen that there is a great scatter of these values. The two parameters can take quite different values even for the same bubble size $R_{M1}$, or intensity of oscillation $p_{zp1}$, and the two quantities are only very weakly correlated. This can be seen in Figure 11, where the variation of the pulse width $\Delta$ with the maximum voltage $u_{M1}$ is shown. The nonlinear regression fit to this data is $<\Delta> = 63.9$ $u_{M1}$ [μs, mV].

Figure 11 can be compared with Figure 8 in [16]. In reference [16] light emission from many bubbles oscillating synchronously in a periodically variable pressure field (the so called acoustic cavitation) has been studied. It can be seen that the scatter of widths $\Delta$ for the measured maximum values $u_{M1}$ is in both figures very similar. This resemblance indicates similarity of the physical processes in both spark-generated bubbles and bubbles oscillating in a variable pressure field, though the latter are generated by a completely different method.

Under the assumption that the glowing plasma core inside the bubble is a spherical blackbody radiator having a radius $R_p$ and a surface temperature $\Theta$, it follows from the Stefan-Boltzman law that the intensity of its radiation at a distance $r$ is given by the equation [37]

$$H_r = \frac{\sigma}{r^2} R_p^2 \Theta^4, \tag{2}$$

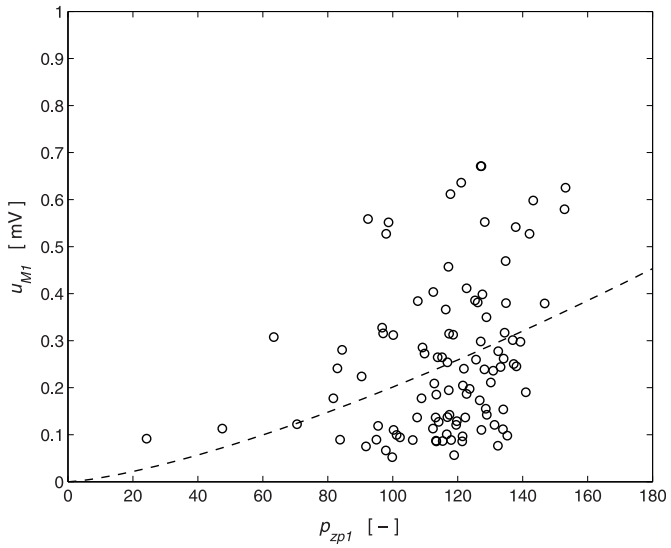


**Fig. 8.** The variation of the maximum voltage in the pulse, $u_{M1}$, with the bubble oscillation intensity, $p_{zp1}$, in dimensionless units.

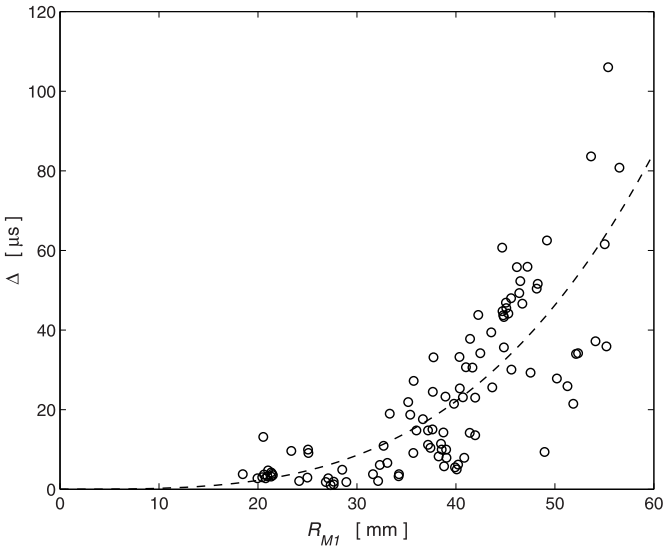


**Fig. 9.** The variation of the pulse width, **Δ**, with the bubble size, $R_{M1}$.

Here $\sigma = 5.67 \times 10^{-8}\,\mathrm{W\,m^{-2}\,K^{-4}}$ and $r = 0.2\,\mathrm{m}$. It can be expected that the assumption of the blackbody radiator is valid in the vicinity of the instant $t_{u1}$ first of all, where the pressure and temperature in the bubble are high. This assumption has been partially experimentally verified in the case of spark-generated bubbles by Golubnichii et al. [25] and in the case of laser-generated bubbles by Brujan et al. [23]. The verification is based on spectral analysis of the light emitted from the bubbles, and it has been found that the spectrum is continuous and can be fitted with the Planck law reasonably well.

It follows from the equation (2) that the intensity of light emitted from the bubble and measured at a distance $r$ depends on a plasma core radius $R_p$ and plasma core surface temperature **Θ**. Let us analyse the experimental data given in Figures 7–10 with respect to these two parameters and with respect to their variation with the bubble size $R_{M1}$ and intensity of oscillation $p_{zp1}$.

Let us first have a look at the variation of the maximum values $u_{M1}$ with the bubble size $R_{M1}$ (Fig. 7). It will be assumed that the highest intensity of the optical radiation (and thus also the maximum voltage $u_{M1}$) occurs at the instant when the bubble is contracted to the first minimum radius $R_{m1}$, that is, it will be assumed that $t_{u1} = t_{c1}$. The plasma temperature at the instant $t_{u1}$ will be denoted as $\mathbf{\Theta}_{M1}$.

As can be seen in the photographs shown in Figure 3, the plasma does not fill the whole volume of the bubble and does not have a precise spherical form. However, again, for the sake of simplicity it will be assumed that both the bubble and the plasma core are concentric spheres of radii $R$ and $R_p$ ($R \geq R_p$), respectively. Let us introduce a quotient $q$ ($q \leq 1$) so that $R_p = q \cdot R$. As can be seen in Figure 3, both the volume of the bubble and of the glowing plasma core is varying during the bubble oscillation and the mutual relation of these two volumes (and thus also the value of $q$) is also varying with time. By observing different bubbles it has also been found that $q$ can take on different values in different experiments even for the same bubble size $R_{M1}$ and intensity of oscillation $p_{zp1}$ [37]. The exact value of $q$ is not known at present. For an interval in the vicinity of $t_1$ (that is, when the bubble radius is close to $R_{M1}$), a mean value $<q_1> = 0.2$ has been used in reference [37]. For an interval close to $t_{c1}$ (that is, when the bubble radius is close to $R_{m1}$), a mean value $<q_{m1}> = 0.8$ is used in [38]. The radius of the maximally contracted plasma can be then expressed as $R_{pm1} = R_{m1} \cdot q_{m1}$.

The bubble minimum radius $R_{m1}$, needed to determine the minimum plasma radius $R_{pm1}$, varies both with the bubble size $R_{M1}$ and bubble oscillation intensity $p_{zp1}$. Let us first consider the variation of $R_{m1}$ and $\mathbf{\Theta}_{M1}$ with $R_{M1}$. Both the quantities should depend on thermal behaviour of bubbles.

Earlier hypotheses concerning thermal behaviour of bubbles have assumed that for sufficiently large bubbles thermal losses are insignificant and therefore the scaling law is valid for these bubbles [39]. The scaling law implies that the temperature $\mathbf{\Theta}_{M1}$ does not depend on the bubble size $R_{M1}$, and varies only with the bubble oscillation intensity. Similarly, the non-dimensional first minimum bubble radius $Z_{m1} = R_{m1}/R_{M1}$ depends only on the bubble oscillation intensity. In these statements the same physical conditions are assumed in experiments, that is, the same liquid, liquid temperature, hydrostatic pressure, etc. The theoretical models used in the computations have assumed ideal gas inside the bubble and adiabatic thermal behaviour of the bubble. The partial plasma content inside the bubble has not been considered yet.

As already said, under the assumption that the scaling law is valid, then for a given oscillation intensity the non-dimensional first minimum radius $Z_{m1}$ is a constant and hence the minimum bubble and plasma core radii $R_{m1}$ and $R_{pm1}$ should be, in the case of the scaling bubbles, directly proportional to the bubble size $R_{M1}$, i.e. $R_{m1} = Z_{m1} \cdot R_{M1}$ and $R_{pm1} = Z_{m1} \cdot q_{m1} R_{M1}$, respectively. And for the scaling bubbles the temperature $\mathbf{\Theta}_{M1}$ should not vary with the bubble size $R_{M1}$. It follows from these relations and from equation (2) that the maximum intensity of light emitted from the bubble should grow with the bubble size as $\sim {R_{M1}}^2$.

However, as can be seen in Figure 7, the experimentally determined maximum intensity of light emitted at the bubble maximum contraction and represented by the voltage $u_{M1}$ grows approximately as $\sim {R_{M1}}^{2.5}$, that is it grows faster than predicted by the theory. Thus the results presented here show that spark-generated bubbles having the sizes $R_{M1}$ ranging from 15 to 55 mm do not behave like scaling bubbles, at least not from the point of view of the temperature $\Theta_{M1}$.

The influence of bubble oscillation intensity on optical radiation is more complex (Fig. 8). Bubble oscillation intensity can influence both $R_{m1}$ (and thus also $R_{pm1}$) and $\Theta_{M1}$. Evidently, a bubble oscillating more intensely is contracted to a smaller minimum radius $R_{m1}$ [39] (and thus also to a smaller $R_{pm1}$), but during this more intensive contraction the pressure at the bubble wall will attain higher values and the bubble content will be more heated. Thus both the maximum pressure and temperature $\Theta_{M1}$ should be higher for more intensely oscillating bubbles. And because the intensity of radiation is increasing with the forth power of $\Theta_{M1}$ and only with the square of $R_{pm1}$, it is evident that a moderate increase of $\Theta_{M1}$ with $p_{zp1}$ will not only overcome the influence of decreasing $R_{pm1}$, but will suffice for a moderate growth of radiation intensity, represented by the maximum voltage $u_{M1}$, which can be seen in Figure 8. Thus it is possible to conclude that the maximum temperature $\Theta_{M1}$ grows only moderately with $p_{zp1}$.

In the case of data shown in Figures 9 and 10 one can proceed in the same way as above. For scaling bubbles the pulse width $\Delta$ should be directly proportional to the bubble size $R_{M1}$ [39] that is the width $\Delta$ should grow as $\sim R_{M1}$. However, as can be seen in Figure 9, the experimentally determined pulse width $\Delta$ is growing with the bubble size as $\sim {R_{M1}}^{3.3}$. At present there is no explanation for this phenomenon.

When analysing the variation of the pulse width $\Delta$ with the oscillation intensity $p_{zp1}$, it has to be said that there are neither experimental nor theoretical data available in literature that could be used as a starting point. Thus the only possibility is to assume a certain analogy between the pressure and light pulses emitted during the first bubble contraction and the following expansion. As far as the pressure pulses $p_1(t)$ are concerned, their peak value $p_{p1}$ is increasing with bubble oscillation intensity and their width is decreasing with bubble oscillation intensity [39]. However, no decrease of the optical pulse width $\Delta$ with the oscillation intensity $p_{zp1}$ can be seen in Figure 10. This further supports the earlier findings that there is only very limited similarity in shape between the pressure pulses $p_1(t)$ and optical pulses $u_1(t)$ (see, e.g., Fig. 3 in [35]) and that plasma in the bubble interior behaves rather autonomously and is only very little influenced by the pressure in the bubble.

At closing this discussion on the variation of the maximum voltage $u_{M1}$ and pulse width $\Delta$ with the bubble size $R_{M1}$ and intensity of oscillation $p_{zp1}$, it should be remarked that the large scatter of the values $u_{M1}$ and $\Delta$ for a given bubble size $R_{M1}$ and bubble oscillation intensity $p_{zp1}$, which can be seen in Figures 7–10, can be due to just relatively small changes of temperature $\Theta_{M1}$ (the temperature influences the intensity of light radiation in the fourth power). Another factor influencing the large scatter of $u_{M1}$ and $\Delta$ may be the shape of the bubble and plasma core at the maximum bubble contraction. In the above discussion only spherical forms were considered. However, real shapes of contracted bubbles may be quite different (see, e.g. photographs in [21]) and thus the intensity of the emitted light may also be influenced by this variation in shape even for the same values of $R_{M1}$ and $p_{zp1}$.

To summarize this analysis, the above discussion shows that with the present state of knowledge it is extremely difficult to interpret the observed data on light emission from oscillating bubbles using the existing theories based on the assumption of ideal gas in the bubble interior. Evidently, further experiments using new methods are needed to throw more light on the complex processes in oscillating bubbles and especially on plasma behaviour.

The measured shapes of the pulses $u_1(t)$ and their widths $\Delta$ can also be compared with data obtained by other researchers. However, this comparison must be done with some caution, as the data from different works have been obtained for different bubbles. For example, spark-generated bubbles are one thousand-time larger than bubbles oscillating in acoustic resonators. Hence, their thermal behaviour is, most probably, very different. Also the initial temperature in laser and spark-generated bubbles is extremely high. On the other hand the initial temperature in bubbles oscillating in acoustic resonators is, most probably, close to the ambient water temperature, at least at the beginning of bubble oscillations. The velocity of the initial energy deposition into a bubble is also different when comparing bubbles generated by low voltage spark discharges with bubbles generated by lasers. However, we believe that the comparison of different bubbles may help in the future in search for a unifying theory.

Let us start with a brief analysis of bubbles excited for oscillation by initially increasing their energy [39]. This class of bubbles encompasses both the spark-generated bubbles and laser-generated bubbles. Golubnichii et al. [26] have already ascertained that according to the velocity of the initial energy delivery into a bubble two kinds of the pulses $u_1(t)$ can be observed (see Figs. 3 and 4 in [26]). In the case of a "slow" energy delivery, as it is during the "low-voltage" discharges used in the work of Golubnichii et al. [26] and in experiments described here, the shape of the pulses $u_1(t)$ is given in Figure 4 and in detail in Figure 5 of this work. On the other hand in the case of a "fast" energy delivery, as it is with "high voltage" discharges described in [26], the form of the pulse $u_1(t)$ is approximately "Gaussian". And the "Gaussian" shape of the pulses $u_1(t)$ has also been observed by researchers studying laser-generated bubbles [21–23].

The pulses $u_1(t)$ recorded in experiments with laser-generated bubbles do not only have the "Gaussian" shape, but their width $\Delta$ increases with the bubble size $R_{M1}$ linearly, that is as $\Delta \sim R_{M1}$, while in this work it has been found to increase as $\Delta \sim {R_{M1}}^{3.3}$. For example Ohl [22] has studied bubbles having the size $R_{M1}$ ranging from 0.6 mm to 1.6 mm and he has observed that the width $\Delta$ was increasing with $R_{M1}$ almost linearly from 4 ns to 9 ns (Fig. 3 in [22]). Baghdassarian et al. [21] studied bubbles with size $R_{M1}$

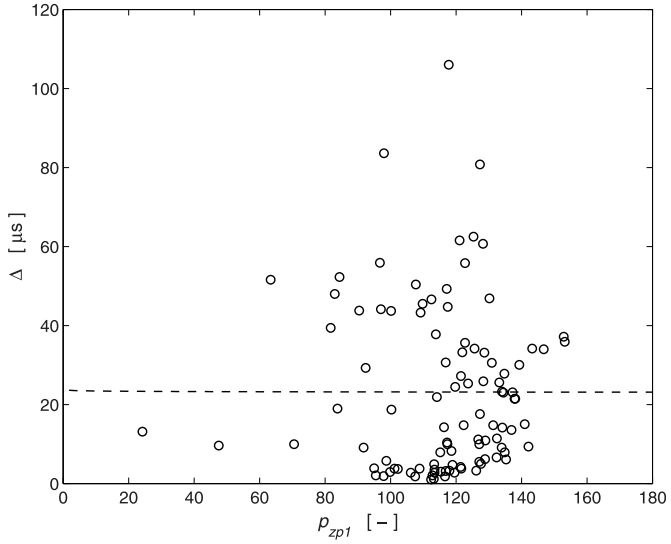


**Fig. 10.** The variation of the pulse width, $\Delta$, with the bubble oscillation intensity, $p_{zp1}$, in dimensionless units.

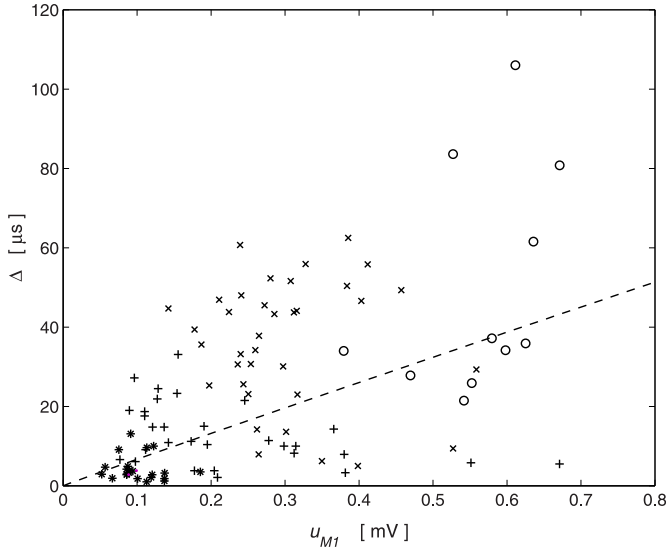


**Fig. 11.** The variation of the pulse width, $\Delta$, with the maximum voltage in the pulse, $u_{M1}$. Bubble sizes: 'o' $R_{M1} > 50$ mm, '×' 50 mm $\geq R_{M1} > 40$ mm, '+' 40 mm $\geq R_{M1} > 30$ mm, '*' 30 mm $\geq R_{M1} > 20$ mm, '.' 20 mm $\geq R_{M1}$.

ranging from 0.2 mm to 0.35 mm and in this case the width $\Delta$ was also increasing with $R_{M1}$ linearly from about 2.1 ns to 3.5 ns (Fig.3 in [21]). Brujan et al. [23] studied bubbles with size $R_{M1}$ ranging from about 0.6 mm to 1.1 mm and the width $\Delta$ was increasing with $R_{M1}$ linearly from about 4.5 ns to 9 ns (Fig. 1 in [23]). For the comparison presented here only data measured under similar laboratory conditions as in this work have been selected (i.e., water at a room temperature $\Theta_\infty \sim 292$ K and hydrostatic pressure $p_\infty \sim 100$ kPa).

The pulse widths $\Delta$ found in this work are compared with the results of Baghdassarian et al. [21], Ohl [22] and Brujan et al. [23] in Figure 12. The nonlinear regression fit to this data is $<\Delta> = 8.1 \times 10^{-3}\ R_{M1}{}^{1.9}$ [s, m]. Together with data obtained in experiments with spark and laser-generated

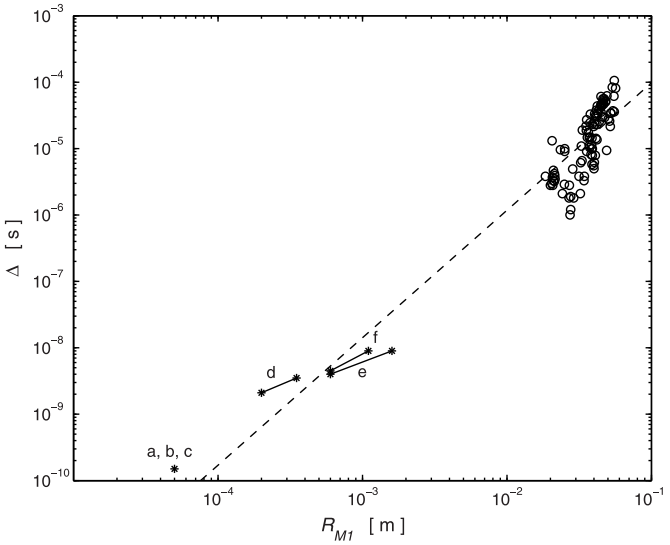


**Fig. 12.** The variation of the pulse width, $\Delta$, with the bubble size, $R_{M1}$: 'o' experimental data obtained in this work, '*' experimental data published in works: 'a' – Gompf et al. [13], 'b' – Moran and Sweider [14], 'c' – Pecha et al. [15], 'd' – Baghdassarian et al. [21], 'e' – Ohl [22], 'f' – Brujan et al. [23].

bubbles also data obtained in studies of single bubbles oscillating in acoustic resonators [13–15] are shown in Figure 12. However, in this case the authors of references [13–15] do not give the bubble size $R_{M1}$. And in works of Gompf et al. [13] and Pecha et al. [15] the pulse width $\Delta$ was determined for a varying driving pressure. To be able to display these data in Figure 12 the value of $R_{M1} = 50$ μm has been used, as this is a typical bubble size for these experiments. And the pulse width $\Delta = 150$ ps has been selected, as this can be considered to be a mean value in the case of the data of these authors.

As already said it is evident that in Figure 12 different sets of data are being compared, that is "slow" energy delivery and "fast" energy delivery into the bubble, as well as free and forced bubble oscillations. Therefore the nonlinear regression fit in Figure 12 has informative character only.

During the experiments described in this work, beside the shape of light pulse, some other phenomena have also been observed. These regard, for example, the difference in instants when the maximum pressure and maximum light from the contracted bubble are radiated [34,35]. Another phenomenon observed is the occurrence of a secondary pulse in $u_1$(t). However, to keep the extent of the present paper in reasonable limits these other phenomena will be discussed elsewhere.

## 5 Conclusions

Due to the large size of experimental bubbles studied in this work, it was possible to observe the shape of the optical pulses radiated during the bubble oscillation in a great detail. It has been found out that the pulses $u_1(t)$ differ in shape from the pulses observed by researchers studying laser-generated bubbles, who have observed a "Gaussian"

shape. Here, during the bubble contraction, the pulse $u_1(t)$ grows relatively slowly to the maximum value $u_{M1}$. However, after reaching the maximum value the optical radiation decreases very rapidly to almost zero. As far as the great scatter of the pulse maximum values $u_{M1}$ and the pulse widths $\Delta$ observed in this work is concerned, it is comparable large as the scatter observed by other researches [21–23]. For example, Ohl [22] reports that "the amplitude varies by 400%" in his experiments (Ohl [22] uses the term "amplitude" for the maximum value $u_{M1}$).

The analysis of the experimental data leads us to a conclusion, which was not provided in earlier works [13–18,21–23], that there are some physical processes in oscillating spark-generated bubbles whose character is still unknown. This conclusion is based on the following observations: (1) The shape of the optical pulses differs substantially from the shape of the acoustic pulses, (2) there is a large scatter of the measured maximum voltages $u_{M1}$ and pulse widths $\Delta$ even for the same bubble size or intensity of oscillations, (3) the quantities $u_{M1}$ and $\Delta$ are only weakly correlated, (4) the scaling law cannot be applied to the maximum surface temperatures of the plasma core, (5) the plasma core behaves autonomously, which follows from the fact that the maximum surface temperatures of the plasma core are only weakly related with the bubble oscillation intensity and thus also only weakly connected with the maximum pressures in the bubble, (6) and at present there is no theoretical explanation for the variation of the mean values $<u_{M1}>$ and $<\Delta>$ with the bubble size and intensity of oscillation. Thus, further experimental data obtained with new methods are needed to throw more light on the complex and so far a bit mysterious processes running in oscillating spark-generated bubbles.

This work has been partly (K.V.) supported by the Ministry of Education of the Czech Republic as the research project MSM 245100304. The authors also wish to thank Prof. J. Picek from the Mathematics Department of the Technical University of Liberec for performing the nonlinear regression fits to the experimental data.

## References

1. A. Shima, K. Takayama, Y. Tomita, N. Miura, Acustica **48**, 293 (1981)
2. A. Jayaprakash, C.-T. Hsiao, G. Chahine, Trans. ASME J. Fluid. Eng. **134**, 031301 (2012)
3. V. Sboros, Adv. Drug Deliver. Rev. **60**, 1117 (2008)
4. E.P. Stride, C.C. Coussios, Proc. Inst. Mech. Eng. J. Eng. Med. **224**, 171 (2010)
5. D.H. Thomas, M. Butler, N. Pelekasis, T. Anderson, E. Stride, V. Sboros, Phys. Med. Biol. **58**, 589 (2013)
6. T. Faez, M. Emmer, K. Kooiman, M. Versluis, A.F.W. van der Steen, N. de Jong, IEEE Trans. Ultrason. Ferroelectr. Freq. Control **60**, 7 (2013)
7. C. Coviello, R. Kozick, J. Choi, M. Gyöngy, C. Jensen, P.P. Smith, C.C. Coussios, J. Acoust. Soc. Am. **137**, 2573 (2015)
8. T.G. Leighton, C.K. Turangan, A.R. Jamaluddin, G.J. Ball, P.R. White, Proc. R. Soc. A **469**, 20120538 (2013)
9. Y. Huang, H. Yan, B. Wang, X. Zhang, Z. Liu, K. Yan, J. Phys. D: Appl. Phys. **47**, 255204 (2014)
10. A.H. Aghdam, B.C. Khoo, V. Farhangmehr, M.T. Shervani-Tabar, Exp. Therm. Fluid Sci. **60**, 299 (2015)
11. Y. Huang, L. Zhang, H. Yan, Z. Liu, K. Yan, IEEE Trans. Plasma Sci. **43**, 3256 (2015)
12. B. Ward, D.C. Emmony, Infrared Phys. **32**, 489 (1991)
13. B. Gompf, R. Günther, G. Nick, R. Pecha, W. Eisenmenger, Phys. Rev. Lett. **79**, 1405 (1997)
14. M.J. Moran, D. Sweider, Phys. Rev. Lett. **80**, 4987 (1998)
15. R. Pecha, B. Gompf, G. Nick, Z.Q. Wang, W. Eisenmenger, Phys. Rev. Lett. **81**, 717 (1998)
16. T.J. Matula, R.A. Roy, P.D. Mourad, J. Acoust. Soc. Am. **101**, 1994 (1997)
17. V.H. Arakeri, A. Giri, Phys. Rev. E **63**, 066303 (2001)
18. I. Ko, H.-Y. Kwak, J. Phys. Soc. Jpn. **79**, 124401 (2010)
19. P.-K. Choi, Y. Sawada, Y. Takeuchi, J. Acoust. Soc. Am. **131**, EL413 (2012)
20. A.G. Akmanov, V.G. Benkovskii, P.I. Golubnichii, S.I. Maslennikov, V.G. Shemanin, Akust. Zh. **19**, 649 (1973) (in Russian)
21. O. Baghdassarian, B. Tabbert, G.A. Williams, Phys. Rev. Lett. **83**, 2437 (1999)
22. C.-D. Ohl, Phys. Fluids **14**, 2700 (2002)
23. E.A. Brujan, D.S. Hecht, F. Lee, G.A. Williams, Phys. Rev. E **72**, 066310 (2005)
24. H.J. Park, G.J. Diebold, J. Appl. Phys. **114**, 064913 (2013)
25. P.I. Golubnichii, V.M. Gromenko, A.D. Filonenko, Zh. Tekh. Fiz. **50**, 2377 (1980) (in Russian)
26. P.I. Golubnichii, V.M. Gromenko, A.D. Filonenko, Zh. Tekh. Fiz. **52**, 1966 (1982) (in Russian)
27. P.I. Golubnichii, V.M. Gromenko, V.M. Krutov, Zh. Tekh. Fiz. **60**, 183 (1990) (in Russian)
28. P.I. Golubnichii, V.M. Gromenko, J.M. Krutov, Dokl. Akad. Nauk SSSR **311**, 356 (1990) (in Russian)
29. Y. Huang, L. Zhang, J. Chen, X. Zhu, Z. Liu, K. Yan, Appl. Phys. Lett. **107**, 184104 (2015)
30. A. Chakravarty, A.J. Walton, J. Lumin. **92**, 27 (2001)
31. N.K. Bourne, J.E. Field, Phil. Trans. R. Soc. Lond. A **357**, 295 (1999)
32. K. Yasui, T. Tuziuti, M. Sivakumar, Y. Iida, Appl. Spectrosc. Rev. **39**, 399 (2004)
33. S. Buogo, K. Vokurka, J. Sound Vib. **329**, 4266 (2010)
34. K. Vokurka, S. Buogo, in *Proceedings of the 36th Jahrestagung für Akustik DAGA 2010*, M. Möser, et al., (ed.) (Deutsche Gesellschaft für Akustik, Berlin, 2010, ISBN: 978-3-9808659-8-2) p. 671, http://kfy.fp.tul.cz/katedra/zamestnanci/vokurka-karel
35. K. Vokurka, S. Buogo, in *Proceedings of the 80th Acoustic Seminar*, M. Brothánek, R. Svobodová, (eds.) (České vysoké učení technické v Praze, Česká akustická společnost, Prague, 2010, ISBN: 978-80-01-04547-3) p. 65, http://kfy.fp.tul.cz/katedra/zamestnanci/vokurka-karel
36. S. Buogo, J. Plocek, K. Vokurka, Acta Acust. United Acust. **95**, 46 (2009)
37. K. Vokurka, J. Plocek, Exp. Therm. Fluid Sci. **51**, 84 (2013)
38. K. Vokurka, Acta Polytech. **57**, 149 (2017)
39. K. Vokurka, J. Sound Vib. **141**, 259 (1990)

**Cite this article as**: Karel Vokurka, Silvano Buogo, Experimental study of light emitted by spark-generated bubbles in water, Eur. Phys. J. Appl. Phys. **81**, 11101 (2018)